IJPSR (2021), Volume 12, Issue 12 (Research Article)

INTERNATIONAL JOURNAL OF PHARMACEUTICAL SCIENCES AND RESEARCH

Received on 03 January 2021; received in revised form, 03 May 2021; accepted, 28 May 2021; published 01 December 2021

ELECTROCHEMICAL DETERMINATION OF ANTI-DEPRESSANT DRUG MIRTAZAPINE EMPLOYING NAFION/f-MWCNTs COMPOSITE AT GLASSY CARBON ELECTRODE

Mahadeva Singh Jat, Varsha Jakhar and D. K. Sharma *

Electrochemical Sensor Research Laboratory, Department of Chemistry, University of Rajasthan, Jaipur - 302004, Rajasthan, India.

Keywords:

Mirtazapine, Anodic adsorptive stripping voltammetry, Functionalized-multiwalled carbon nanotubes, Voltammetry, Glassy carbon electrode

Correspondence to Author:
D. K. Sharma

Electrochemical Sensor Research Laboratory, Department of Chemistry, University of Rajasthan, Jaipur - 302004, Rajasthan, India.

E-mail: sharmadkuor@gmail.com

ABSTRACT: A nafion plus functionalized-multiwalled carbon nanotubes modified glassy carbon electrode (f-MWCNTs/GCE) was developed for the determination of anti-depressant drug mirtazapine (MIR). The electro-chemical behavior of the molecule was investigated employing cyclic voltammetry (CV), chronocoulometry (CC), and differential pulse adsorptive stripping voltammetry (DPASV). The surface morphology of the electrodes has been studied through scanning electron microscopy (SEM). These studies revealed that the oxidation of MIR is facilitated at f-MWCNTs/GCE. After optimization of analytical conditions employing this electrode at pH 10.5 of 0.04M carbonate buffer for MIR, the peak currents were found to be linearly with different concentrations in the range of 6.72×10^{-6} M to 3.74×10^{-4} M for MIR. The detection limits were obtained of 32.45×10^{-8} M and 9.45×10^{-7} M for MIR, using DP-AAdSV. The prepared modified electrode has several advantages, such as simple in preparation method, showed high sensitivity with very low detection limits, and gave excellent reproducibility. The proposed method was also employed for the determination of MIR in pharmaceutical formulations, urine and blood serum samples.

INTRODUCTION: Mirtazapine (1,2,3,4,10,14b-hexahydro-2-methyl pyrazino [2,1-a] pyrido[2,3-c] benzazepine) structure is given in Scheme-1, which is a tetracyclic piperazinoazepine and has a different structure from any other currently used anti-depressant. It enhances central noradrenergic and serotonergic activity by blocking α2 receptors as well as selectively antagonizing 5HT2 and 5HT3 receptors. MIR is well absorbed without regard to food intake. It demonstrates about linear kinetics over its usual dosage range and reaches a peak plasma level approximately two hours after an oral dosage.

QUICK RESPONSE CODE

DOI: 10.13040/IJPSR.0975-8232.12(12).6442-52

This article can be accessed online on www.ijpsr.com

DOI link: http://dx.doi.org/10.13040/IJPSR.0975-8232.12(12).6442-52

It is metabolized in the liver via the P450 cytochrome oxidase pathway. Plasma protein binding is ~ 85%. The N-desmethyl metabolite is pharmacologically active. Elimination occurs via 75% urine and 15% feces. Clearance of the drug is diminished in the presence of liver or renal impairment.

Therefore, a lower dosage is recommended in the elderly and patients with liver or renal disfunction [1-5]. Various analytical methods have been used to determine the MIR in various samples, such as liquid chromatography [6-11], spectrofluorimetry & spectrophotometry [12-15] and electrochemical [1]. A survey of the literature reveals that no electrochemical data are exactly available concerning the voltammetric behaviour similar to the present work for MIR. Moreover, no monograph of MIR has been reported in the official pharmacopeia's as of today with no any similarity

with this report. Electroanalytical methods have proved to be highly sensitive to the analysis of drugs in pharmaceutical dosage forms and biological samples due to their straight forwardness, low cost and relatively short analysis time compared to the other analytical techniques [16-20]. Voltammetric techniques are most suitable for investigating the redox properties of active drug compounds. This can give insight into the metabolic fate, *in-vivo* redox process or pharmaceutical activity [21-23]. Owing to the widespread use of the LC-UV method in routine analysis, it is important that specific and validated LC methods are used for the analysis of an active drug compound in its pharmaceutical dosage form. LC-UV methods offer important advantages, such as low cost, and have proven to be a valuable method in the quality control of active drug substances. The first purpose of the present study was to carry out a detailed investigation about the voltammetric behaviour and analysis of MIR at carbon-based electrodes using cyclic, linear sweep (LS), and pulse voltammetric techniques. Secondly, the determination of MIR using RP-LC techniques with a stability test was performed as per ICH norms.

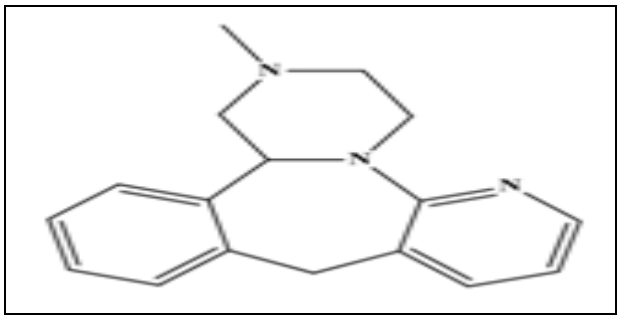

SCHEME 1: THE CHEMICAL STRUCTURE OF MIRTAZAPINE

MATERIALS AND METHODS:

Chemicals: Mirtazapine was purchased from a local pharmacy under the trade name Remeron (Apotex). A standard stock solution of 2.7×10^{-4} M MIR in bulk was prepared in methanol solvent and preserved at 5 ºC until assessment. A series of carbonate buffers of pH values 9.0 to 12.0 was prepared and used as a supporting electrolyte with KCl solution. Deionized water was used to prepare all the solutions during experiments. The working solutions were prepared by a fixed volume of stock solution and buffers. Analytical grade reagents were used.

Instrumentation: Employment for electrochemical techniques model 1230A [SR 400] electrochemical analyzer (CHI Instrument TX, USA), with a totally automated attached to a PC with proper CHI 100W version 2.3 software for total control of the experiments, treatment, and data collection. A conventional three-compartment cell was used for the voltammetric experiments.

The working electrode was a 5 mm diameter GCE inserted into a glass tube. The electrode was polished thoroughly with alumina and cleaned in an ultrasonic bath before each measurement. The counter electrode was a platinum wire. The reference electrode is Ag/AgCl (1M KCl). A digital pH-meter (CHINO-DB-1011) fitted with a glass electrode standardized with buffers of known pH was used for measuring the pH values of the solutions.

Preparation of f-MWCNTs Suspension and GCE Modification: 4 mg MWCNTs were acidified with 4 mL of a mixture of acid (HNO_3:H_2SO_4) in the ratio of 1:3 respectively, for 2 hrs and acidified CNTs were washed with water until removed water gets pH 7.0. These activated CNTs were dried and then dispersed in the mixture of 2 mL N,N-dimethylformamide + 0.5 ml nafion (a conducting polymer, 0.5% ethanol) and diluted with water followed by hot sonication for 4 hrs in an ultrasonic bath to get homogeneous suspension. 15 µL of this suspension was allowed to drop onto the pre-treated GCE surface using a micropipette and left at room temperature to dry.

General Procedure: For a total 11 ml solution, carbonate buffer of pH 10.5 and the appropriate concentration of the MIR were introduced into the electrochemical cell and purged with pure deoxygenated nitrogen for 10-15 min under stirred conditions. These results to remove oxygen gas before measurements. Electrochemical pre-treatment was always performed in the same solution in which the measurement was subsequently carried out. The working glassy carbon electrode was polished 0.05 µm aluminium-oxide and sonicated for a short time to remove impurities on the electrode surface, and then it was dried in an oven at 45 ºC. After optimization of operational parameters, the cyclic and stripping voltammograms were recorded.

For voltammetric analysis of MIR, appropriate quantities of the analyte solution were placed into a 25 mL standard volumetric flask and then diluted to the mark with 0.04 M carbonate buffer of pH 10.5. The solution was then transferred into the electrochemical cell, where the measurements were carried out.

A magnetic stirrer (Expo Hi-Tech, India) with a stirring bar was used to provide the convective transport of the analyte during its accumulation onto the GCE surface. For MIR, an accumulation potential of 0.8 V was applied to the f-MWCNTs/GCE for 200 s while the solution was stirred with the magnetic stirrer. At the end of the accumulation period, the stirring was stopped, and a 15 s rest period was allowed for the solution to become quiescent.

The voltammogram was then recorded by scanning the potential towards the positive direction from 0.6 to 1.4 V for VF using the differential pulse mode employing a step potential of 5 mV and modulation amplitude of 50 mV. When necessary, renewal of the electrode surface was easily accomplished by soaking the modified electrode into the supporting electrolyte and cycling the potential between 0.4 V and 1.4 V (*vs.* Ag/AgCl) in carbonate buffer (pH 10.5) solution five times before use so as to renew the electrode surface.

The cyclic voltammetric experiments were carried out by scanning the potential from 0.6 V to 1.4 V for MIR. Double potential step chronocoulometry was carried out with a pulse period of 10 s from 0.6 V to 1.4 V for MIR vs. Ag/AgCl. The SEM images were obtained by removing the surface layers of bare GCE and f-MWCNTs/GCE from their respective electrode and dropping on carbon-coated aluminum grids for SEM imaging since the modified electrodes could not be inserted directly into the SEM.

Treatment and Determination of Samples: Analysis of MIR was carried out in pharmaceutical formulations and synthetic samples. Ten tablets of MIR were weighed and ground to a fine powder using a mortar and pestle. For all of these experiments, the samples were diluted to 9 mL with pH 10.5 of carbonate buffer solution. Recovery tests were performed for the determination of MIR by spiking standard solutions of these molecules into pharmaceutical formulations.

The urine and blood serum samples were collected from healthy volunteers. For the determination of MIR in urine samples, no pre-treatment step was carried out. Blood serum samples were obtained from a local pathology clinic and stored under refrigeration. To avoid interferences occurring from the serum matrix, a 1 mL serum sample was added to the electrochemical cell containing 9 mL of buffer solution.

RESULTS AND DISCUSSION:

Morphological Characterization of the f-MWCNTs/GCE: Scanning electron micrographs' (SEM) were used for the morphological studies of f-MWCNTs modified surface of GCE using a ZEISS-EV018 instrument at the University Science and Instrumentation Centre in the University of Rajasthan, Jaipur. The CNTs can be seen in the scanning electron micrograph covering the surface area of bare glassy carbon electrode **Fig. 1**.

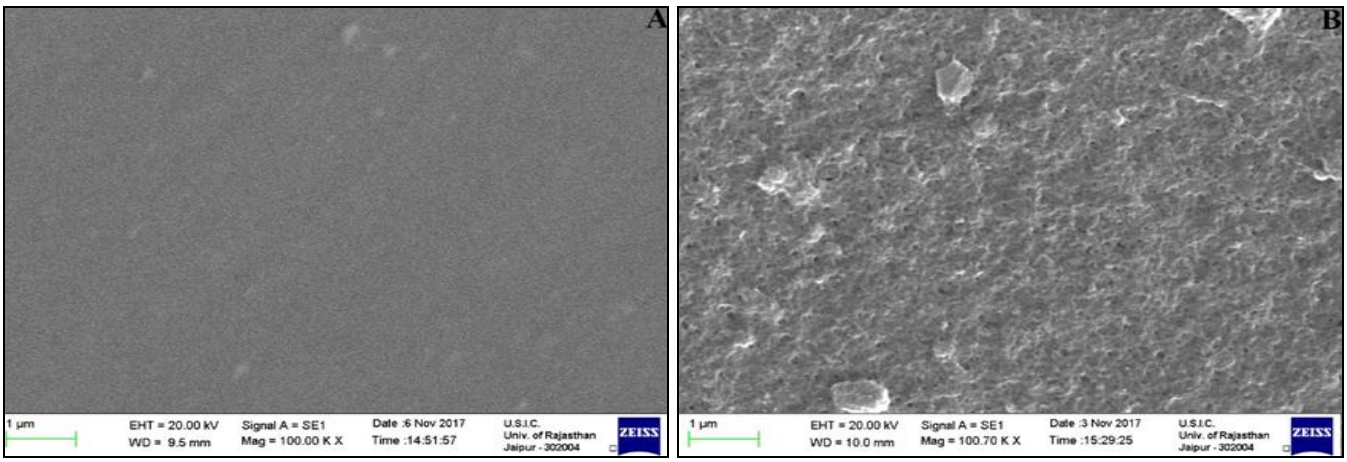

FIG. 1: SEM IMAGES (A) BARE GCE (B) F-MWCNTS NAFION MODIFIED SURFACE OF GCE

The doping of the bare GCE resulted into grate improvement in the peak response due to the increased surface area and better electron transfer rate between electrode and electrolyte interface.

It is well documented that the modification of electrode surface by the f-MWCNTs increase anodic peak current Ip can be calculated by the expression (equation-1) [26-27].

$$Ip = (2.69\times10^{5})\, n^{3/2}\, A\, C_o\, D_o^{1/2}\, \nu^{1/2} \ldots\ldots\ldots\ldots (1)$$

For $K_4[Fe(CN)_6]$, n = 1 and D = 7.6×10^{-6}. From the slope of the Ip versus $\nu^{1/2}$ relation, the microscopic areas are found to be 0.0443 cm^2 for the bare GCE and 0.0892 cm^2 for the f-MWCNTs/GCE electrodes. Evidently, the modified electrode had increased in surface area of nearly 84%.

Effect of pH: Standard solutions of 2.7×10^{-4} M MIR were used to find the optimum pH of the supporting electrolyte best suited for their determination by GCE employing CV, square wave voltammetry (SWV) and differential pulse voltammetry (DPV).

The influence of the pH on the oxidation peaks currents of MIR was investigated in the pH range of 9.0-12.0, employing the carbonate buffer.

It was observed that as the pH of the medium was gradually increased, the potential shifted towards more positive values which suggesting the involvement of protons and electrode in the reaction. Below pH 9.0 there are no oxidation peaks observed for MIR.

From the plot of Ep versus pH for MIR **Fig. 2B**, it was observed that a slope of 0.058 V **Fig. 2B** was obtained in the pH range of 9.0-12.0, which is indicative of an equal number of electrons and protons being involved in the oxidation of MIR. The lone pair of electrons in the tertiary nitrogen of MIR is more easily oxidized than that in aromatic ring. However, preferential oxidation of aromatic pi-electrons in MIR takes place as the nitrogen present in the side chain has no other group for stabilization after the loss of electrons.

Whereas the loss of an electron from an aryl ring produces radical cation, which can be stabilized by the nitrogen attached to the ring. Thus, the probable oxidation mechanisms of MIR are given in Scheme-2. For MIR, the electron transfer occurs in two steps.

It was also observed that the peak current (IP) reached its maximum value at pH 10.5 for MIR oxidation. Thus, this pH was employed for further studies. Various buffers, such as phosphate, carbonate, and B.R. buffer, were then employed at pH 10.0 for MIR.

Out of all the buffer's pH the pH 10.5 was optimized. Carbonate buffer gave the best response in terms of peak current and peak shape for MIR and; hence, these media were employed for all further experiments. In the next step, optimization of buffer concentration was carried out by varying its concentration in the range of 0.03-0.2 M. The best peak response was observed for 0.04 M Carbonate buffer for MIR and therefore these concentrations were used for all further studies.

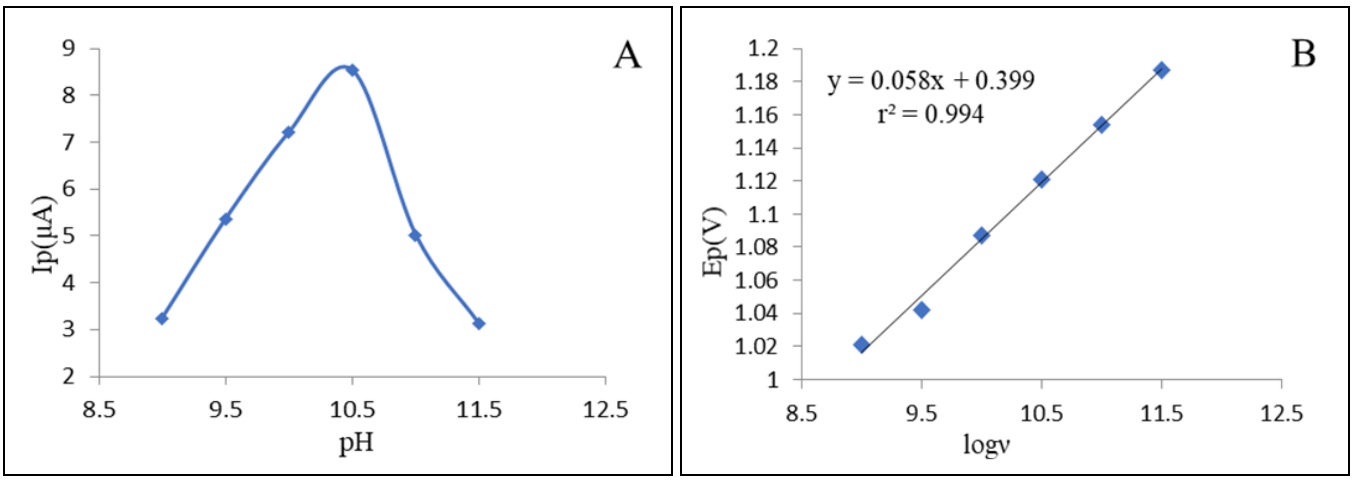

FIG. 2: PLOT OF PEAK CURRENT VERSUS PH (A) AND PLOT OF PEAK POTENTIAL VERSUS LOGARITHM OF SCAN RATE (B) FOR MIR IN 2.7×10^{-4} M IN CARBONATE BUFFER OF PH 10.5

Cyclic Voltammetry: Effect of Scan Rate: The effect of scan rate (ν 1/2) on peak current (IP) was examined under the above experimental conditions. As the sweep rate is increased from 20 to 200 mV/s at a fixed concentration of MIR, the peak potential shifted towards a more positive value with an increase in current, confirming the irreversible nature of the reduction process [21] **Fig. 3**.

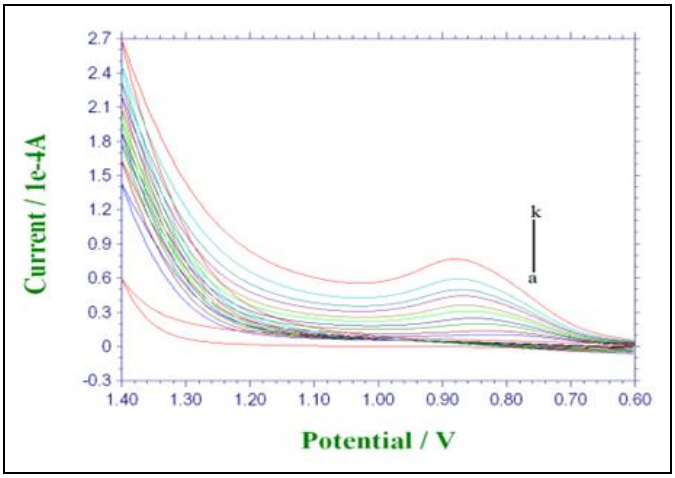

FIG. 3: CYCLIC VOLTAMMOGRAMS AT DIFFERENT SCAN RATES OF 2.7×10^{-4} M MIR: (A) BLANK, (B) 20 MV/S, (C) 40 MV/S, (D) 60 MV/S, (E) 80 MV/S, (F) 100 MV/S, (G) 120 MV/S, (H) 140 MV/S, (I) 160MV/S, (J) 180 MV/S, (K) 200 MV/S AT PH 10.5 IN CARBONATE BUFFER

On subsequent scans (i) the peak potential shift anodically and (ii) the peak current function, IP(μA)/ν1/2 exhibits almost constancy, where A is the cross-sectional area of electrode in cm^2, C is the concentration of MIR in mol/L. When peak current (Ip) was plotted against square root of scan rate (ν) a straight line was obtained as following (equation-2) the Garrido equation [24-25].

$$I_P = (1.06\times10^6)\, n^2\, A\, C_o\, D_o^{1/2}\, \nu\, t_p^{1/2} \ldots\ldots\ldots (2)$$

Where n is the number of electrons exchanged in oxidation, n' is the number of electrons involved in the rate determining step of the electrode process, α is the charge transfer coefficient, A (cm^2) is cross sectional area of the electrode, Co (mol/cm^3) is the concentration of the electro-active species in the bulk solution, Ip (μA) is the anodic peak current, Do ($cm^2\ s^{-1}$) is the diffusion coefficient of the electro active species being reduced and ν (Vs^{-1}) is the scan rate [22, 23].

A linear Randles–Sevcik plot (plot of Ip versus $\nu^{1/2}$) as shown in **Fig. 4A** is obtained, indicating (equation-3) that the diffusion is the means of mass transport [26-27].

$$Ip\ (\mu A) = 0.0089\ ^{\nu 1/2}(mV/s) + 0.89;\ r^2 = 0.988\ldots\ldots (3)$$

The finding was further confirmed by plotting log Ip versus log ν **Fig. 4B**; a straight line was observed which can be expressed by the equation (equation-4):

$$\log Ip\ (\mu A) = 0.462 - 0.0275 \log \nu(mV/s);\ r^2 = 0.996\ldots\ldots\ldots(4)$$

The obtained slope of 0.462 is close to 0.5 also confirms diffusion-controlled nature of the electrode process.

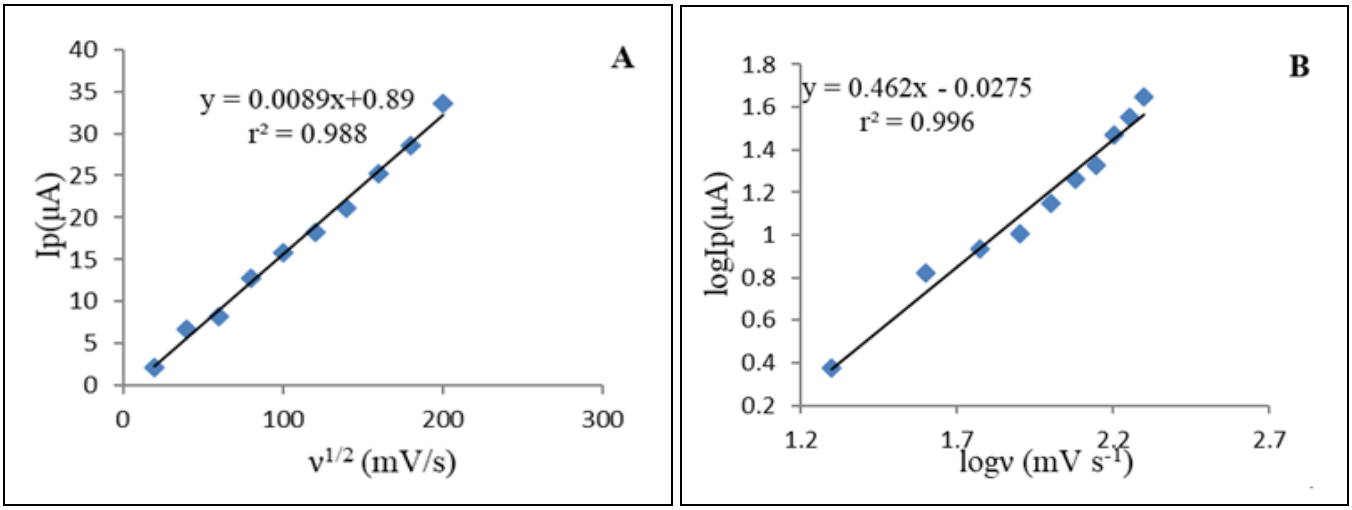

FIG. 4: PLOT OF PEAK CURRENT (I_P) VERSUS SCAN RATE (N) FROM VOLTAMMOGRAMS OF FIGURE-3 FOR 2.7×10^{-4} M MIR CONCENTRATION IN CARBONATE BUFFER OF PH 10.5 (A) AND PLOT OF LOGARITHM PEAK CURRENT VERSUS LOGARITHM OF SCAN RATE (B)

Kinetics of Oxidation of Mirtazapine:

Determination of Parameter [αn'] and Heterogeneous Electrochemical Rate Constant (ks): For the diffusion-controlled oxidation kinetics, the value of αn^' and heterogeneous electrochemical rate constant (ks) was calculated by the Laviron,s equation [28-29]. The slope and intercept of graph Ep versus log ν **Fig. 5B** following that the slope and intercept are equal to $2.303RT/2\alpha n'F$ and E^o- $RT/\alpha n'F$ [0.78 + ln($D_o^{1/2}/k_s$) -0.5 ln$RT/\alpha n'F$] according to the equation-5.

$$Ep = Eo - RT / an F [O\ 0.78 + In\ (D1 / 2/o/k_s)\text{-}05\ In\ RT / anF] - (RT/ 2anF)\ 1nv$$

Where α is the transfer coefficient, ν the scan rate, n the number of electrons transferred, k_0 the standard heterogeneous rate constant of the reaction, and E_0 is the formal redox potential. R, T, and F have their usual meanings.

Thus αn' was easily calcu lated to be 1.075 from the slope of Ep versus log ν [24]. The plot between Ep versus ν is also given in **Fig. 5A**.

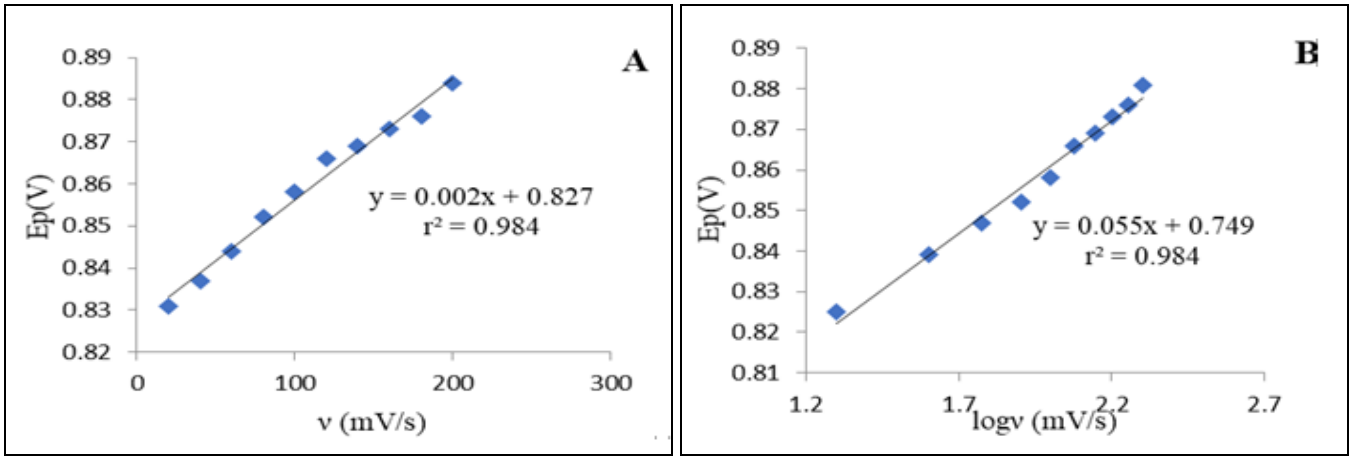

FIG. 5: PLOT OF PEAK POTENTIAL (E_P) VERSUS SCAN RATE (N) FROM VOLTAMMOGRAMS OF FIGURE-3 FOR 2.7×10^{-4} M MIR CONCENTRATION IN CARBONATE BUFFER OF PH 10.5 (A) AND PLOT OF PEAK POTENTIAL VERSUS LOGARITHM OF SCAN RATE (B)

Straight-line of Ep versus log ν plot is expressed by the following linear regression as shown in equation-6:

$$E_p = 0.055 \log \nu + 0.749;\ r^2 = 0.984 \ldots\ldots\ldots(6)$$

The value of αn' and heterogeneous electro-chemical rate constant (ks) was calculated by comparing slope, and intercept of equations-5 was found equal to 1.075 and 1.795.

Determination of Total Number of Electrons: The total number of electrons (n) involved in the overall oxidation process was calculated by analyzing the charge consumed by the desired concentration of MIR. This was accomplished by taking 5 mL of 4 mg mL^{-1} solution of MIR in a cell and electrolysis was performed at a potential of 1.121 against Ag/AgCl reference electrode for10 hours. During the electrolysis, solutions were kept stirred and purged with nitrogen. Due to long-time electrolysis, current efficiency and completion of electrolysis were assumed to be nearly 100% and 99.98%, respectively. The total number of electrons (n) involved in overall oxidation process was calculated using the formula Q = nFN, where Q is charge in coulombs, N is number of moles of MIR and F is Faraday's constant. The value of n was found to be 2 for MIR at f-MWCNTs/GCE [30-32].

Determination of Diffusion Coefficient (Do in cm^2/s) and Surface Coverage (Γ^O): Electro-oxidation of 2.7×10^{-4} M MIR at the bare GCE and f-MWCNTs/GCE was investigated by employing chronocoulometry for the determination of the kinetics and mechanisms of electrode reactions. Employing double-potential step chrono-coulometry, after point-by-point background subtraction, the plot of charge (Q) versus the square root of time ($t^{1/2}$) showed a linear relationship. According to the integrated Cottrell equation (equation-8), the diffusion coefficient and Qads of MIR could then be estimated from the slope and intercept, respectively, of the plot of total Q versus $t^{1/2}$, given by the Anson equation [32-35]. The resulting calculated parameters are presented in **Table 2**. As can be seen from the table, the value of the slope

and the Qads for the f-MWCNTs/GCE were more than that for other electrodes, confirming that NAF along with CNTs makes the accumulation of MIR onto the electrode surface more effective. The surface coverage (Γ^O) for all four electrodes was calculated using the following relationship [31] (equation-7) and the results are given in **Table 2**.

$$Q_{ads} = nFA\Gamma^O \text{…….(7)}$$

From these values, it was observed that the maximum surface coverage is observed in the case of the f-MWCNTs/GCE.

Thus, due to the synergistic effect of f-MWCNTs, the electrode surface coverage by MIR drastically increased, and the kinetics of oxidation became more facile, confirming the results obtained from CV.

Integrated Cottrell equation $Q_d = (2nFAD_O^{(1/2)} C_O t^{(1/2)}/ \pi^{1/2}$ ……(8)

Electroanalytical Determination of MIR: Since voltammetric methods have cost-effectiveness, high accuracy, precision, sensitivity, and absence of lengthy extraction processes, therefore, they are widely used for analytical purposes. In the present paper, differential pulse voltammetry and differential pulse anodic adsorptive stripping voltammetric technique was optimized for the determination of MIR in bulk form, human serum and in human urine at GCE [36-37].

Optimization of Parameters: Operational parameters such as accumulation time (t_{acc}), accumulation potential (E_{acc}), scan increment (ΔS), peak to peak amplitude, pulse amplitude (Esw), pulse period and pulse width, *etc.* [38] were optimized before recording DP-AAdS voltammograms to get the best response in terms of peak shape, peak current, peak height, and peak stability. The optimized parameters are given in **Table 1**.

TABLE 1: THE OPTIMIZED EXPERIMENTAL PARAMETERS OF DP-AADSV AND DPV PROCEDURES

Optimized operational parameters	for DP-AAdSV	Optimized operational parameters	for SW-AAdSV
Scan increment (mV)	04	Scan increment (mV)	05
Pulse amplitude (mV)	50	Pulse amplitude (mV)	50
Deposition time (s)	15	Deposition time (s)	16
Deposition potential (V)	0.0	Deposition potential (V)	0.0
Pulse width (s)	0.2	Pulse width (s)	0.3
Pulse period (s)	0.5	Pulse period (s)	0.4

Effect of Concentration: In order to determine the effect of concentration of MIR on SW-AAdSV and DP-AAdSV peak current, voltammograms of MIR are recorded at MWCNTs/GCE **Fig. 6A** and **B**. The linearity evaluated by linear regression analysis was calculated by the least square regression method [39-40].

The calibration curve constructed for MIR is linear over the concentration 4.25×10^{-6} to 3.74×10^{-4} M for SW-AAdSV and 6.72×10^{-6} to 3.25×10^{-4} M for DP-AAdSV method.

Since the differential pulse, anodic adsorptive stripping voltammetry (DP-AAdSV) is more sensitive than square wave anodic adsorptive stripping voltammetry, (SW-AAdSV) detailed studies are carried out using differential pulse anodic adsorptive stripping voltammetry. The calibration curves (**Fig. 7A** and **B**) were represented by the following equations-9 and 10:

DP-AAdSV: Ip (μA) = (46525) C (M) + (17.20); $r^2 = 0.993$; n = 2 …….(9)

SW-AAdSV: Ip (μA) = (42851) C (M) + (13.45); $r^2 = 0.994$; n = 2 …….(10)

The regression plots showed that there was a linear dependence of the current intensity on the concentration in both DP-AAdSV and SW-AAdSV modes over the range given in **Table 3**.

Detection and Quantification Limit: Detection limit is calculated by equation LOD= 3 SD/b, where SD is the standard deviation of intercept and b is the slope of the regression line. The calculated LOD values of mirtazapine are 54.23×10^{-8} g/mL for DP-AAdSV and 32.45×10^{-8} g/mL for SW-AAdSV method. The quantitation limit (LOQ) is examined by the equation LOQ= 10 SD/b. These values are 17.25×10^{-7} g/mL for DP-AAdSV and 9.45×10^{-7} g/mL for SW-AAdSV method [41].

Application of Analytical Determination to Spiked Human Serum and Urine Samples: The significance of the proposed method was examined by employing it for the determination of mirtazapine in spiked blood as a biological sample [42] without any requirement of time-consuming extraction or evaporation step for sample preparation the proposed method can be applied simply after dilution step with direct measurements in acidic media. Results of the analytical study of spiked blood are summarized in **Tables 4** and **5**.

TABLE 2: COMPARABLE ELECTROCHEMICAL BEHAVIOUR OF 2.7×10^{-4} G/ML MIR DETERMINED AT BARE GCE AND F-MWCNTS/GCE

Electrolyte	E_p/V (Ag/AgCl)	I_p/µA	D_o (cm^2/s)	k_o (s^{-1})	I^o
MIR at bare GCE	1.12	2.652	4.26×10^{-4}	0.767	5.24×10^{-3}
MIR at f-MWCNTs/GCE	0.98	30.34	7.45×10^{-4}	1.795	105.24×10^{-3}

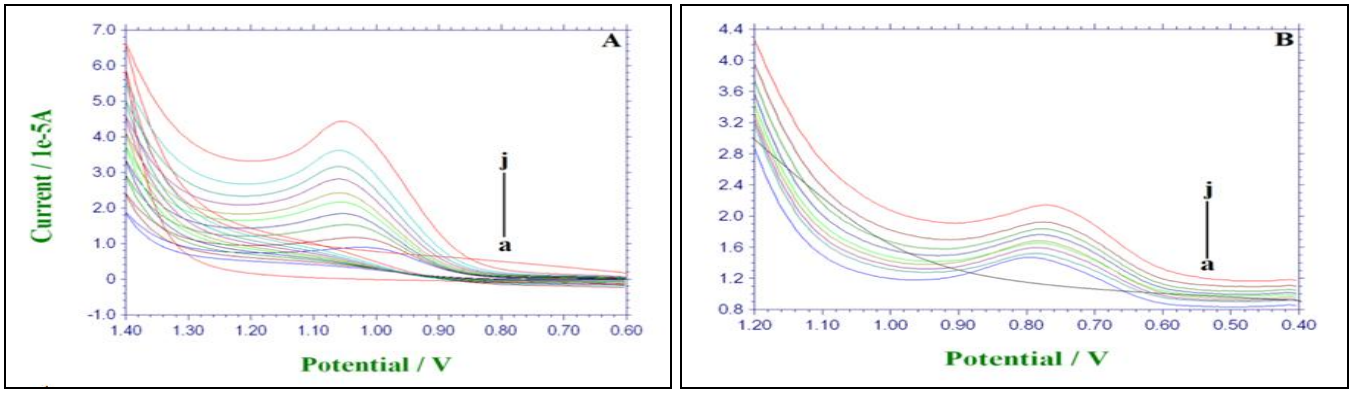

FIG. 6: THE DEPENDENCE OF THE DIFFERENTIAL PULSE ANODIC ADSORPTIVE STRIPPING VOLTAMMOGRAM PEAK CURRENT (IP) OF 2.7×10^{-4} MOL/L MIRTAZAPINE WITH DIFFERENT CONCENTRATIONS AT F-MWCNTS/GCE; PH 10.5 (A) BLANK, (B) 1.0×10^{-4} G/ML, (C) 1.3×10^{-4} G/ML, (D) 1.5×10^{-4} G/ML, (E) 1.7×10^{-4} G/ML, (E) 1.9×10^{-4} G/ML, (G) 2.1×10^{-4}G/ML, (H) 2.3×10^{-4} G/ML AND (I) 2.5×10^{-4} G/ML (A) AND THE DEPENDENCE OF THE SQUARE WAVE ANODIC ADSORPTIVE STRIPPING VOLTAMMOGRAM PEAK CURRENT (IP) OF 2.7×10^{-4} MOL/L MIRTAZAPINE OF DIFFERENT CONCENTRATIONS AT F-MWCNTS/GCE; PH 10.5 (A) BLANK, (B) 0.6×10^{-4}G/ML, (C) 0.8×10^{-4}G/ML, (D) 1.0×10^{-4} G/ML, (E) 1.2×10^{-4} G/ML, (E) 1.4×10^{-4} G/ML, (G) 1.6×10^{-4} G/ML, (H) 1.8×10^{-4} G/ML AND (I) 2.0×10^{-4} G/ML (B)

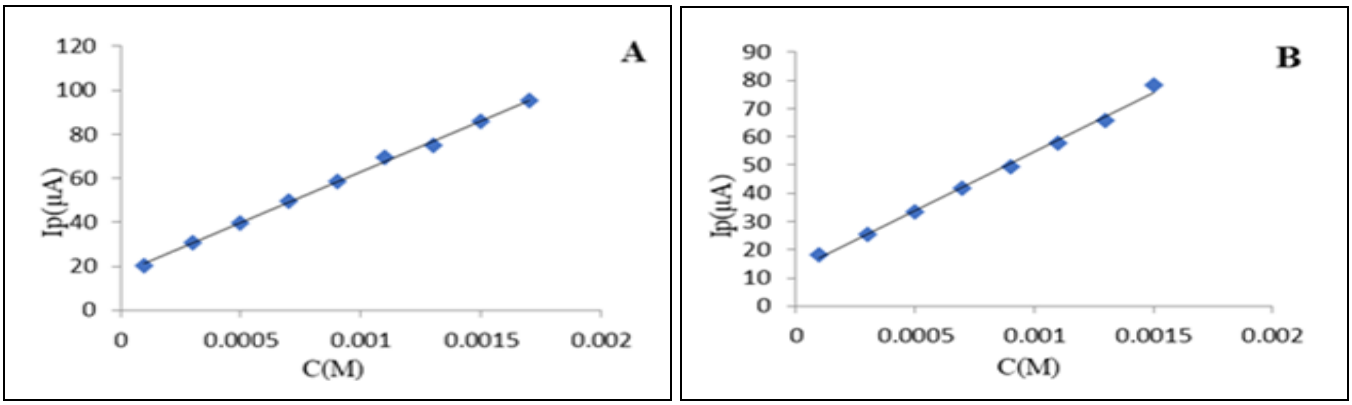

FIG. 7: CALIBRATION PLOTS: PEAK CURRENT VERSUS C(M) IN SW-AADSV (A) AND PEAK CURRENT VERSUS C(M) IN DP-AADSV TECHNIQUE (B) AT F-MWCNTS/GCE

TABLE 3: ANALYTICAL PARAMETERS FOR VOLTAMMETRIC ANALYSIS OF MIRTAZAPINE USING DP-AADSV AND SW-AADSV TECHNIQUES

Techniques	Concentration range	Regression equation	r^2	LOD	LOQ	S.D.
SW-AAdSV	4.25×10^{-6}-3.74×10^{-4} M	I_p(µA) = (42851) C(M) + 13.45	0.994	32.45×10^{-8}g/mL	9.45×10^{-7}g/mL	9.64×10^{-4}
DP-AAdSV	6.72×10^{-6}-3.25×10^{-4}M	I_p(µA) = (46525) C(M) + 17.20	0.993	54.23×10^{-8}g/mL	17.25×10^{-7}g/mL	8.36×10^{-4}

TABLE 4: RECOVERY RESULTS OF PROPOSED METHOD FOR SPIKED HUMAN SERUM SAMPLES (SOLUTION OF STANDARD MIR WAS SPIKED)

Sample	Amount added, mg/L	Amount found, mg/L	Recovery[a]	%RSD
Standard in serum sample	10	10.03 9.78 10.01 9.98 9.98	9.656 ± 0.44 t_{cal} = 2.742 t_{tab} = 2.785	1.44

[a]Results of recovery values are given as mean ± ts/_n (at 97% confidence level)

TABLE 5: RECOVERY RESULTS OF PROPOSED METHOD FOR SPIKED HUMAN URINE SAMPLES (SOLUTION OF MIR WAS SPIKED)

Sample	Amount added, mg/L	Amount found, mg/L	Recovery[a]	%RSD
Standard in urine sample	10	9.97 9.85 9.78 10.1 9.96	9.95 ± 0.54 tcal 1.781 ttab = 2.31	1.67

[a]Results of recovery values are given as mean ± ts/_n (at 96% confidence level)

Proposed Oxidation Mechanism of MIR: On the basis of pH, CV, and CPC studies, it was concluded that 2 electrons and 2 protons were participating in the oxidation process of MIR.43 Herein, the oxidation mechanism was proposed based on all the experimental observations (Scheme 2):

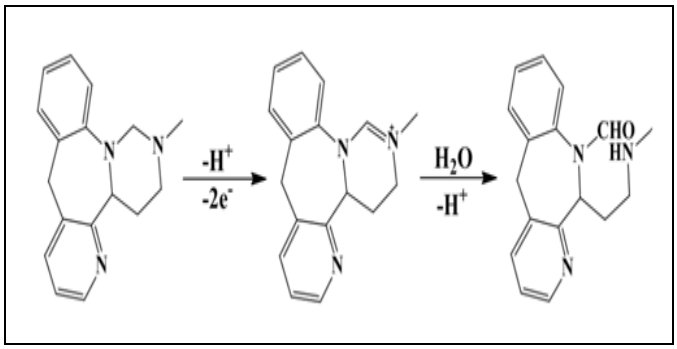

SCHEME 2: PROPOSED OXIDATION MECHANISM OF MIR

CONCLUSION: Electrochemical behaviour of antidepressant medication MIR was studied at modified glassy carbon electrode, using CV, DPV, DP-AAdSV and SW-AAdSV techniques, in bulk formulation. It was found that the oxidation process of MIR was irreversible, diffusion-controlled, and pH-dependent. Furthermore, kinetic parameters such as diffusion coefficient (Do), number of electrons (n), and electron transfer coefficient (ks) were also calculated, which were used to propose an oxidation mechanism. DP-AAdSV and SW-AAdSV method was employed for the determination of MIR in a blood sample as a biological sample. The proposed method is direct, simple, cost-effective, requires only small amount of analyte and does not involve tedious steps such as separation, filtration, extraction, evaporation *etc.*, required by chromatographic methods [44]. Furthermore, the proposed method has good operational characteristics such as extremely low values of detection limits, sensitivity, selectivity, wide liner working range, and it exhibits good accuracy, precision, & repeatability for the determination of mirtazapine in bulk, urine as well as in serum as a biological sample.

ACKNOWLEDGMENT: One of the authors (Mahadeva Singh Jat) is thankful to the Council of Scientific and Industrial Research, New Delhi, India, by grant File Number 09/149(0685)/2016/ EMR-I.

CONFLICTS OF INTEREST: There are no conflicts to declare.

REFERENCES:

1. El-Shal MA: A copper oxide nanoparticle modified screen-printed electrode for determination of mirtazapine. Egyptian Journal of Chemistry 2019; 62(9):1739-48.
2. Nutt D: Mirtazapine: pharmacology in relation to adverse effects. Acta Psychiatrica Scandinavica 1997; 96: 31-37.
3. Hartmann PM: Mirtazapine: a newer antidepressant. American Family Physician 1999; 59: 159-61.
4. Ottman AA, Warner CB and Brown JN: The role of mirtazapine in patients with fibromyalgia: a systematic review. Rheumatology International 2018; 38:2217-2224.
5. Kessler DS, MacNeill SJ, Tallon D, Lewis G and Peters TJ: Mirtazapine added to SSRIs or SNRIs for treatment resistant depression in primary care: phase III randomised placebo controlled trial (MIR). BMJ 2018; 363: 4218.
6. Hong X, Yao Y, Hong S and Lei C: LC-MS-MS analysis of mirtazapine in plasma and determination of

pharmacokinetic data for rats. Chromatographia 2008; 68: 65-70.
7. Mandrioli R, Mercolini L, Ghedini N, Bartoletti C, Fanali S and Raggi MA: Determination of the antidepressant mirtazapine and its two main metabolites in human plasma by liquid chromatography with fluorescence detection. Analytica Chimica Acta 2006; 556: 281-88.
8. Pistos C, Koutsopoulou M and Panderi IA: A validated liquid chromatographic tandem mass spectrometric method for the determination of mirtazapine and dimethyl mirtazapine in human plasma: application to a pharmacokinetic study. Analytica Chimica Acta 2004; 514: 15-26.
9. Ptacek P, Klima J and Macek J: Determination of mirtazapine in human plasma by liquid chromatography. Journal of Chromatography B: Analytical Technologies in the Biomedical and Life Sciences 2003; 794: 323-28.
10. Romiguieres T, Pehourcq F, Matoga M, Begaud B and Jarry C: Determination of mirtazapine and its demethyl metabolite in plasma by high-performance liquid chromatography with ultraviolet detection: Application to management of acute intoxication. Journal of Chromatography B: Analytical Technologies in the Biomedical and Life Sciences 2002; 775: 163-68.
11. Labat L, Dallet P, Kumer E and Dubost JP: Spectro-photometric, spectrofluorimetric, HPLC and CZE determination of mirtazapine in pharmaceutical tablets. Journal of pharmaceutical and biomedical analysis 2002; 28: 365-71.
12. Saini B, Kaushal M and Bansal G: A validated direct spectrofluorimetric method for quantification of mirtazapine in human whole blood. Spectroscopy 2010; 24: 641-49.
13. Youssef RM: Determination of mirtazapine in spiked human plasma and tablets by first derivative spectrofluorimetric method. Saudi Pharm J 2010; 18: 45-49.
14. Kumar DR, Lakshmi VN, Vardhan SVM and Rambabu C: Determination of mirtazapine in tablet dosage forms by visible spectrophotometry. Biosciences Biotechnology Research Asia 2008; 5: 863-66.
15. Karaşen N and Altinöz S: Determination of mirtazapine in tablets by UV spectrophotometric and derivative spectrophotometric methods. Journal of Pharmaceutical and Biomedical Analysis 2000; 24: 11-17.
16. Uslu B and Ozkan SA: Electroanalytical application of carbon-based electrodes to the pharmaceuticals. Analytical Letters 2007; 40:817-53.
17. Uslu B and Ozkan SA: Solid electrodes in electroanalytical chemistry: Present applications and prospects for high-throughput screening of drug compounds. Combinatorial Chemistry and High Throughput Screening 2007; 10: 495-13.
18. Uslu B, Ozkan SA and Aboul-Enein HY: Analysis of pharmaceuticals and biological fluids using modern electroanalytical techniques. Critical Reviews in Analytical Chemistry 2003; 33: 155-81.
19. Symth MR and Vos JG: Analytical Voltammetry. Vol. XXVIII of series, Comprehensive Analytical Chemistry, Amsterdam 1992.
20. Goyal RN, Chatterjee S and Rona ARS: A single wall carbon nanotubes modified edge plane pyrolytic graphite sensor for determination of methylprednisolone in biological fluids. Talanta 2009; 80: 586-92.
21. Wang J: Electroanalytical Techniques in Clinical Chemistry and Laboratory Medicine. VCH, New York 1988.
22. Wang C, Guan J, Qu Q, Yang G and Hu X: Voltammetric determination of sinomenine in biological fluid using a glassy carbon electrode modified by a composite film of polycysteic acid and carbon nanotubes. Combinatorial Chemistry & High Throughput Screening 2007; 10: 595-03.
23. Uslu B, Ozkan SA and Aboul-Enein HY: Electrochemical study of S-adenosyl-L-methionine and its differential pulse and square wave voltammetric determination. Electroanalysis 2002; 14: 736-40.
24. Garrido L: On the covariance of the Fokker-Planck equation. Physica A: Statistical Mechanics and Its Applications 1980; 100(1): 140-52.
25. Garrido J: Thermodynamics of electrochemical systems. The Journal of Physical Chemistry B 2004; 108(47): 18336-40.
26. Zanello P: Inorganic electrochemistry: theory, practice and application. The Royal Society of Chemistry 2003.
27. Allen AJ, Bard, Larry R and Faulkner: Electrochemical methods: fundamentals and applications. (2nd ed.) John Wiley & Sons 2001.
28. Laviron E: Theoretical study of a 1e-, $1H^+$ surface electrochemical reaction (four-member square scheme) when the protonation reactions are at equilibrium. Journal of Electroanalytical Chemistry and Interfacial Electrochemistry 1980; 109: 57-67.
29. Laviron E: General expression of the linear potential sweep voltammogram in the case of diffusionless electrochemical systems. Journal of Electroanalytical Chemistry and Interfa Electrochemi 1979; 101(1): 19-28.
30. Nicholson RS: Theory and application of cyclic voltammetry for measurement of electrode reaction kinetics. Analytical chemistry 1965; 37(11): 1351-55.
31. Jakhar V, Jhankal KK and Sharma DK: A novel electrochemical sensing of 8-hydroxy-5-nitro-quinoline moiety using graphene-oxide fabricated glassy carbon electrode. Analytical Chemistry Letters 2019: 9: 430.
32. Hong J, Zhao Y-X, Xiao B-L, Moosavi-Movahedi AA, Ghourchian H and Sheibani N: Direct electrochemistry of hemoglobin immobilized on a functionalized multi-walled carbon nanotubes and gold nanoparticles nanocomplex-modified glassy carbon electrode. Sensors 2013; 13(7): 8595-11.
33. Anson FC, Christie JH and Osteryoung RA: A study of the adsorption of cadmium(II) on mercury from thiocynate solutions by double-potential step chronocoulometry. Journal of Electroanalytical Chemistry 1967; 13: 343-52.
34. Anson FC, Rebert and Osteryoung RA: Chrono-coulometry: A convenient, rapid and reliable technique for detection and determination of adsorbed reactants. Journal of Chemical Education 1983; 60(4):293.
35. Anson FC: Innovations in the study of adsorbed reactants by chronocoulometry. Analytica Chem 1966; 38(1): 54-57.
36. Fotouhi L: Electrochemical behaviour and voltammetric determination of sulfaguanidine at a glassy carbon electrode modified with a multi-walled carbon nanotubes. International Journal of Electrochemical Science 2012; 7:3919-28.
37. Elqudaby HM: Validated voltammetric method for the determination of some antiprotozoa drugs based on the oxidation at an activated glassy carbon electrode. Arabian Journal of Chemistry 2013; 6:327-333.
38. Kissinger PT and Heineman WR: Laboratory techniques in electroanalytical chemistry. Marcel Dekker: New York 1996.
39. Sharma DK, Mourya GL, Jhankal KK, Jones LA and Bhargava SK: Electrochemical behaviour and validated

determination of the anticancer drug. Tamoxifen, Der Pharma Lett 2012; 4(5): 708-14.
40. Uslu B and Ozkan SA: A rapid HPLC assay for the determination of lamivudine from pharmaceuticals and human serum. Analytica Chimica Acta 2002; 462:49.
41. Ozkan SA: Electroanalytical methods in pharmaceutical analysis and their validation. 1st ed., HNB Pub 2011.
42. Riley CM and Rosanske TW: Development and validation of analytical methods. Elsevier, Amsterdam, the Netherlands 1996.
43. Jat MS, Meena K, Jhankal KK and Sharma DK: Sensitive electro-chemical determination of antidepressant drug clomipramine at f-MWCNTs nano clusters modified glassy carbon electrode. J Pharm Sci & Res 2019; 11(3): 700-07.
44. Jat MS, Jakhar V, Jhankal KK and Sharma DK: electrochemical determination of anesthetic drug ropivacaine in pharmaceutical formulations by differential pulse cathodic adsorptive stripping voltammetry. Chemical Science Transactions 2019; 8(1): 28-35.

How to cite this article:
Jat MS, Jakhar V and Sharma DK: Electrochemical determination of anti-depressant drug mirtazapine employing nafion/f-mwcnts composite at glassy carbon electrode. Int J Pharm Sci & Res 2021; 12(12): 6442-52. doi: 10.13040/IJPSR.0975-8232.12(12).6442-52.